The Pennsylvania State University

The Graduate School

Department of Meteorology

THE DURATION AND MAGNITUDE OF FRESHWATER FLOODING EVENTS 11.4 AND 13.0 ka BP AS INFERRED FROM PALEO-SALINITY VARIATIONS IN THE CHAMPLAIN SEA

A Thesis in

Meteorology

by

Brandon G Katz

Submitted in Partial Fulfillment
of the Requirements
for the Degree of

Master of Science

May 2009

The thesis of Brandon G Katz was reviewed and approved* by the following:

Raymond Najjar
Associate Professor of Meteorology and Geosciences
Thesis Advisor

Michael Mann
Associate Professor of Meteorology and Geosciences

William Brune
Professor of Meteorology
Head of the Department of Meteorology

*Signatures are on file in the Graduate School

ABSTRACT

Freshwater fluxes into the North Atlantic are known to have caused catastrophic shifts in climate by weakening the formation of North Atlantic Deep Water (NADW). During the end of the last glacial period, several large freshening events were recorded in the geologic record within the Champlain Sea, indicating that large volumes of freshwater from pro-glacial lakes, such as Lake Agassiz and others in the Great Lakes Region, likely routed out into the North Atlantic. This study utilizes a two-dimensional estuarine model of the Champlain Sea during two flood events at 11.4 and 13.0 ka BP to estimate the durations and magnitudes of these freshwater flooding events, the later being of particular note as it closely predates the Younger Dryas cooling episode. Values of pre and post-flood paleo-salinity within the current-day Lake Champlain are used as constraints within the model to determine the amount and duration of freshwater fluxes required to cause the observed salinity changes. Paleo-salinity during the 11.4 ka BP event changed from 25 ppt to 8 ± 3 ppt, which requires flood volumes in excess of 5,500 km^3 to inundate the region over timescales of less than two weeks. The model could not reproduce the observed freshening of the Champlain Sea (25 to 0 ± 3 ppt) for reasonable flood volumes, which may reflect model limitations in strongly sloping bathymetry and narrow channels, as well as uncertainties in the bathymetric reconstruction. These constraints on the fluxes of freshwater into the North Atlantic are useful in understanding what may have caused partial or total shutdowns of NADW during the end of the last ice age.

TABLE OF CONTENTS

LIST OF FIGURES

LIST OF TABLES

ACKNOWLEDGEMENTS

I would like to thank my advisors Dr. Raymond Najjar, Dr. Thomas Cronin, and Dr. Michael Mann; my collaborators Dr. John Rayburn, Dr. David Franzi, and Dr. Peter Knuepfer; and my funding source, the USGS. In addition, I would like to thank the Northeast Section of the Friends of the Pleistocene for allowing me to take a geologic field trip through my study area. I would like to thank my friends and family for providing support and tolerance over the duration of this research project. And finally, I would like to thank Katie for putting up with me and loving me unconditionally, even when grumpy.

Chapter 1

Introduction

During the last glacial-interglacial cycle, the advance and retreat of the Laurentide Ice sheet (LIS) reshaped the land in the Northern United States and much of Canada. Of particular note is the final retreat wherein the southern margin of the ice sheet melted, inundating large regions of low-laying land area with melt-water. The largest of these freshwater bodies are referred to as pro-glacial lakes. The largest pro-glacial lake was Lake Agassiz, which over its 5000-year history covered up to 1.5 million km^2 (Leverington and Teller 2003, Teller and Leverington 2004). During most of its lifetime, Lake Agassiz was bordered to the north by the LIS, which supplied a constant source of melt-water. Over this time period other lakes, such as Lake Algonquin, occupied the current-day Great Lakes region with drainage routes open to the current-day Gulf of St. Lawrence after approximately 13,100 years before present (13.1 ka BP). These pro-glacial lakes have a complex history governed by rainfall, variable melt-water rates, and the opening of various outlet channels. Figure 1.1 shows this lake-system as it was 11.5 ka BP.

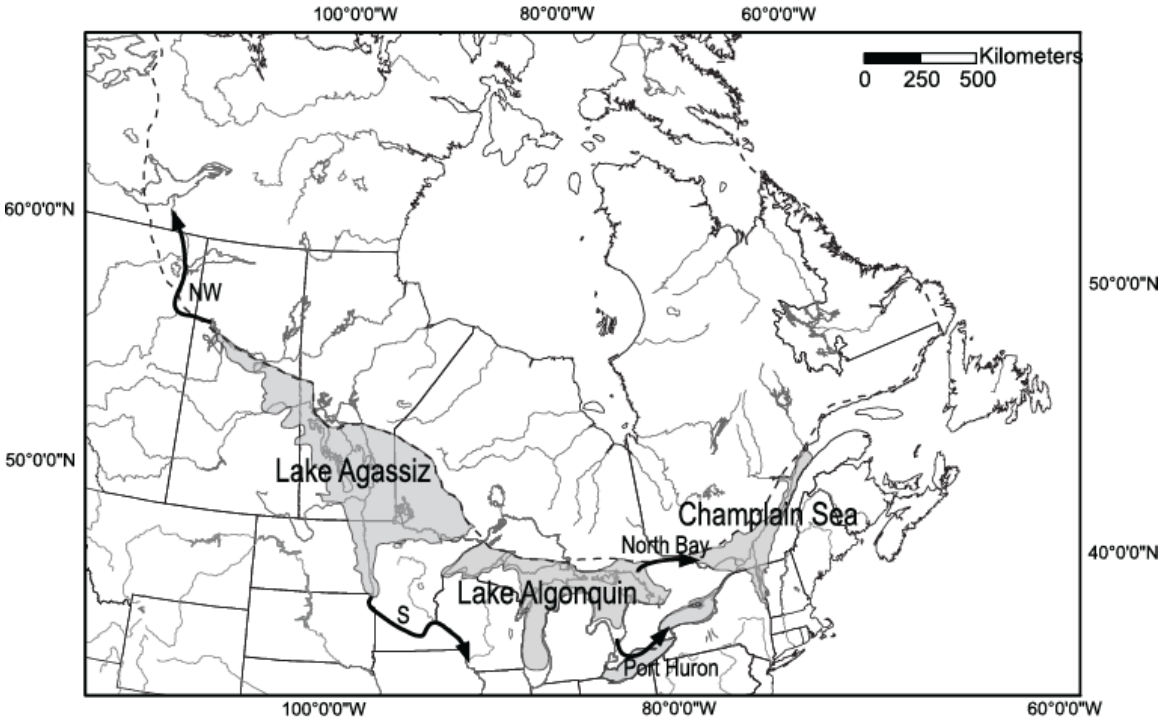

Figure **1.1**: Map of the pro-glacial lake system around 11.5 ka BP. The dashed line represents the southern boundary of the LIS, while the darker grey portions depict the water-bodies, and arrows delineate theorized drainage routes (Teller and Leverington 2004, Cronin et al. 2008a).

At various times in the history of Lake Agassiz the LIS receded northward, opening outlets to regions of lower elevation through which large amounts of freshwater could escape to the ocean. Some of these freshwater events are theorized to have been catastrophic, with floods often scouring out deep gorges and valleys. Five major flood routes have been proposed (fout of which are shown in figure 1.1): southward through the current-day Mississippi River Valley to the Gulf of Mexico, one through the Mackenzie River Valley to the Arctic Ocean, one through Hudson Bay and Hudson Strait into the North Atlantic Ocean, and two to the North Atlantic through the Hudson and St. Lawrence River Valleys (Leverington and Teller, 2003). Paleo-climate models indicate that these flood events are likely important catalysts of abrupt climate change due to their ability to freshen surface ocean waters. Freshening these waters

can drastically alter major ocean circulation patterns, including the formation of North Atlantic Deep Water (NADW). For example, freshwater injected to the North Atlantic can have major repercussions on the ocean's Meridional Overturning Circulation (MOC) (Ganopolski and Rahmstorf 2001), which plays an important role in the climate system. However, the timing, magnitude and location of these flood events, critical factors for how they influence ocean circulation and climate, are not well constrained (Lowell et al. 2005).

The Champlain-St. Lawrence Valley has long been viewed as the outlet route for several flood events, including that which may have caused the onset of the Younger Dryas cooling event about 13.0 ka BP (Broecker et al. 1989). After the emergence of pro-glacial lakes in this region (Lakes Vermont, Iroquois, and Candona), along with the subsequent opening of the current day St. Lawrence Seaway, the Champlain Sea was formed (see figure 1.1 for the location of the Champlain Sea as defined in this study). During the period after the drainage of Lake Vermont between 13.0 and 9.0 ka BP, the isostatically depressed region that contained the Champlain Sea was known to exhibit many of the characteristics of a modern day estuary, wherein salty waters are known to have intruded substantially into the Champlain-St. Lawrence Valley. Recently, new paleo-environmental reconstructions from sediment cores obtained in the current-day Lake Champlain are providing evidence for several deglacial freshwater inflow events from 11.4 and 13.0 ka BP into the Champlain Sea (Cronin et al. 2008a). Studies such as those by Rayburn et al. (2005, 2006) and Franzi et al. (2007) confirm extensive work carried out over the last few decades (e.g. Rodrigues, 1988, Rodrigues and Vilks 1994) that glacial lake water quickly drained from the St. Lawrence-Champlain-Ontario basins into the North Atlantic. These events likely signify drainage from Lake Agassiz or other glacial lakes in the modern Great lakes region into the Champlain Sea.

The present study utilizes a 2-dimensional estuarine model of the Champlain Sea to estimate the flood volumes and durations responsible for the paleo-salinity changes inferred from the sediment cores by Cronin et al. (2008a). The study will focus on two events at 11.4 and 13.0 ka BP (Franzi et al. 2007, Cronin et al. 2008a, Rayburn et al. in press, Cronin et al. 2008b), corresponding to the two largest freshening events in the sediment records. The 13.0 ka BP event is of particular interest as it closely predates the onset of the Younger Dryas cooling event and is marked by the largest paleo-salinity change in the core records (larger floods exist toward the end of Lake Agassiz's lifetime). Although the magnitude of the freshening events can be estimated, the resolution of the core data is such that it is difficult to discern sub-annual changes. This study will examine the sub-annual changes and provide best-estimates as to the duration of the flood events. The flood magnitudes and durations found in this study may then be used in paleo-climate modeling to better understand the overall picture of the flood pulses that moved through the Champlain Sea and into the world ocean.

Chapter 2

Model and Observational Constraints

This chapter describes the model, its inputs, and its application toward quantifying salinity and flow variations caused by pro-glacial flooding of the Champlain Sea.

2.1 The Estuarine Model

The estuarine model used in this study is a 2-dimensional (over depth and along the axis of flow) dynamic model of flow velocity and salinity variation developed by MacCready (2007). A brief description is provided here. The model is essentially a time-dependent version of the equations of Hansen and Rattray (1965), which are integrated using forward-time and centered-space derivatives as described by Press et al. (1992). Tidal characteristics from real-world estuaries are then used to optimize a tidal mixing parameterization. The model gives reasonable salinity and flow profiles for San Francisco Bay, Hudson Bay, and several other estuaries (MacCready 2007).

Required inputs to the model are bathymetry, daily averaged tidal velocity at the mouth of the estuary, freshwater influx at the head, and salinity at the ocean boundary. The model assumes a simplified bathymetry in which the cross section is rectangular. In this configuration, the depth is equal to the maximum depth and the width is computed in order to maintain the observed cross-sectional area. Resolution for the model is 20 km along the axis of the estuary and continuous in the vertical. The time step is variable, adjusting to flow changes in order to maintain numerical stability while minimizing computational expense.

2.2 The Bathymetry

In order to create the bathymetric profiles for the 11.4 and 13.0 ka BP flooding events, several sources of information are combined: Nautical Charts of the current-day St. Lawrence Seaway, a Digital Elevation Model (DEM) of the St. Lawrence Region, DEM reconstructions of the Champlain Sea Region during the two events, and the location of the southern boundary of the Laurentide Ice Sheet.

The nautical charts are obtained from the Defense Mapping Agency and Hydrographic/Topographic Center in Bethesda, MD (Appendix). The maps display high-resolution ship soundings of depth from Mean Low Low Water (MLLW), which can easily be read and transcribed into a data file. These charts are used instead of digital sources because of their higher resolution (10 m depth spaced contours compared to 2 km blocks). To determine where to sample depth information, a transect is overlaid running from the mouth of the waterway at 65^{o} W to Quebec City, Qc (71^{o} W). At intervals of 20 km, lines are drawn perpendicular to the primary flow axis from the center of the waterway to the coasts. Data are then recorded at 7.5 km intervals from the north coast to the south coast. In more variable bathymetry or where the width is less than 75 km, the resolution is increased by progressively halving the 7.5 km spacing so that at least ten points are present in each cross-section. The finest spacing used is 0.9375 km.

Elevation above water level around the St. Lawrence is derived from the current-day DEM of the St. Lawrence region, obtained from the National Geophysical Data Center (Amante et al. 2008). The flow axis and perpendicular transects are again overlaid on the DEM with the location of the north and south coasts (the limits of the nautical charts) plotted. Readings are then taken to the north and south of the coasts at the same resolution as the nautical chart

transects. In order to link the current-day DEM with the nautical charts, readings are taken at each perpendicular transect's coastlines and the DEM is then corrected to the nautical chart. Figure 2.1 depicts this method.

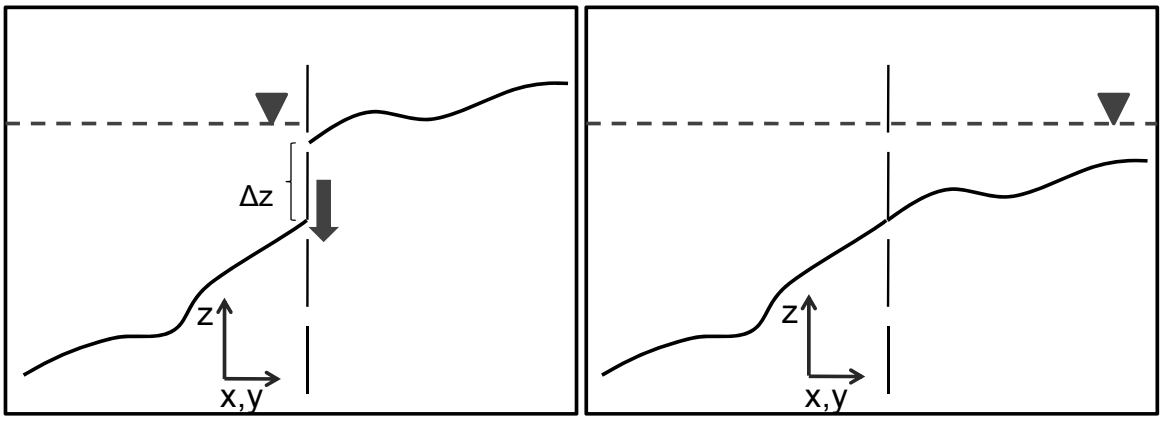

Figure **2.1**: Graphical depiction of map correction technique. One relative profile is assumed to be "correct," while the other is assumed to require an adjustment to the "correct" level. The difference between the profiles at the overlapping point, Δz, is subtracted from the second profile.

Performing the above operation for each perpendicular transect allows the creation of a single consistent topographic and bathymetric data set for the current day St. Lawrence Region. Because of the weight of the LIS, the Champlain-St. Lawrence Valleys were isostatically depressed during the time periods of interest, 11.4 and 13.0 ka BP. Furthermore, global mean sea level was lower than today due to the sequestration of water in continental ice sheets. From 11.4 to 13.0 ka BP, deglaciation had proceeded approximately halfway from the last glacial maximum (LGM), leading to global sea-level rise from a low of -125 m (with respect to the present day) during the LGM (Pirazzoli and Pluet 1991) to about -60 ± 10 m near 13.0 ka BP (Peltier and Fairbanks 2006).

To account for the elevation differences due to isostatic adjustment, a reconstructed DEM (referred to as a paleo-DEM throughout) of the western portion of the Champlain Sea for

each time period is obtained from Rayburn et al. (2005). They used modern DEMs, paleo-strandlines (ancient beaches and deltas that determine coastlines), and isostatic rebound lines to produce the differentially depressed topography and bathymetry of the western Champlain Sea. By selecting a point on these DEMs that is closest and overlapping to the St. Lawrence Region (the most northeast corner of each DEM), the same operation depicted in figure 2.1 is performed to correct the current-day combined topography/bathymetry of the St. Lawrence Region to the time period of interest. The water level of Rayburn et al. (2005) is then used for the combined DEM. This corrected DEM will now be referred to as the Modified Period DEM (MPD).

The primary flow axis and transects are now extended from Quebec City, Qc to 75^{o} W in the Champlain Sea. For perpendicular transects that overlap both the Paleo-DEM and the MPD (i.e. that run northward outside of the boundary defined by the northern border of the paleo-DEM), the operation depicted in figure 2.1 is used to correct the portion of the transect within the MPD to the portion of the transect within the paleo-DEM. After adjusting the overlapping transects, the location of the LIS must be considered as it may form sections of the waterway's northern boundary. The latitudes and longitudes of the ice sheet boundaries are obtained from Dyke et al. (2008) and subsequently drawn onto the DEM, with the 11,000 and 10,000 radiocarbon years BP maps used for the 13.0 and 11.3 ka BP events, respectively (Rayburn et al. 2005). Figure 2.2 depicts the resultant bathymetry for 11.4 and 13.0 ka BP with the axial flow and perpendicular transects overlaid.

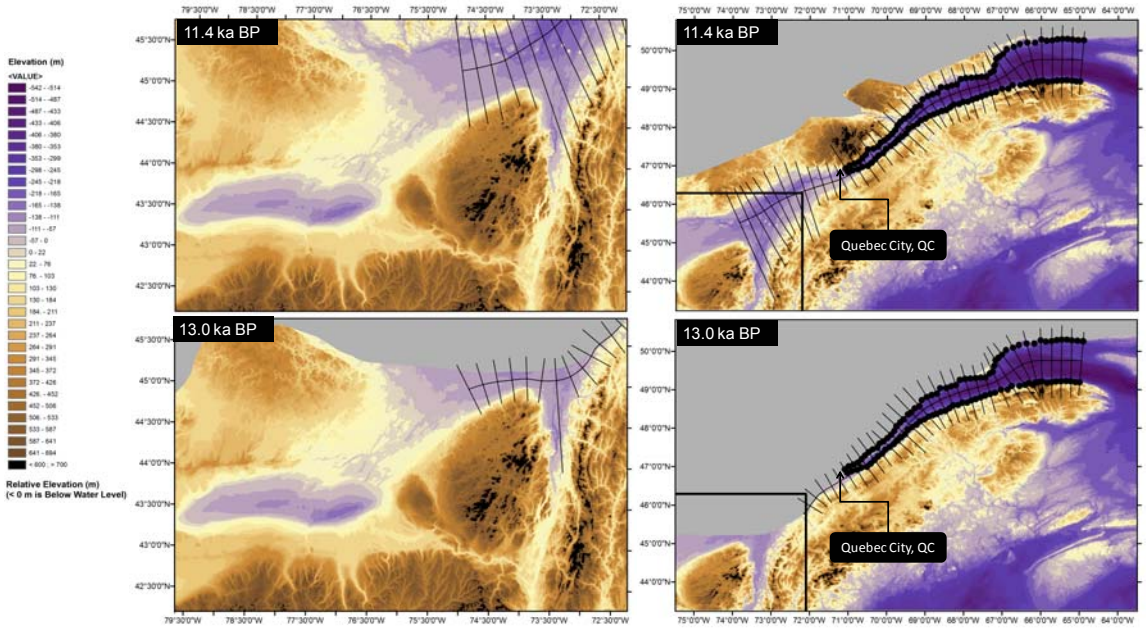

Figure **2.2**: Upper Left: 11.4 western Champlain Sea DEM; Upper Right: 11.4 MPD; Bottom Left: 13.0 ka BP western Champlain Sea DEM; Bottom Right: 13.0 ka BP MPD. The transects along the middle of the estuaries represent the primary axis of flow while the perpendicular transects represent the discrete 20-km spaced cross-sections where depths and elevations are recorded. The black dots on the two right hand-side images represent the coast line of the current day nautical charts. The partial black box visible in the southwestern corner of each MPD is the outline of the western Champlain Sea DEM (the area covered by the left side images). The darker grey boundary to the north represents the location of the ice sheet.

There is now a uniform bathymetric data set that may be used to determine the maximum depth and cross-sectional area along the axis of primary flow. The area under water is first calculated using trapezoidal integration. Because the model requires that the depth for each rectangle be the maximum depth of the cross section, the area is divided by maximum depth to obtain the width of each cross section. Performing the aforementioned analysis yields estuaries with volumes of 8.45×10^5 and 5.97×10^5 km^3 for the 11.4 and 13.0 ka BP cases, respectively. Figure 2.3 displays the along-axis cross-sectional areas of the 11.4 and 13.0 ka BP scenarios.

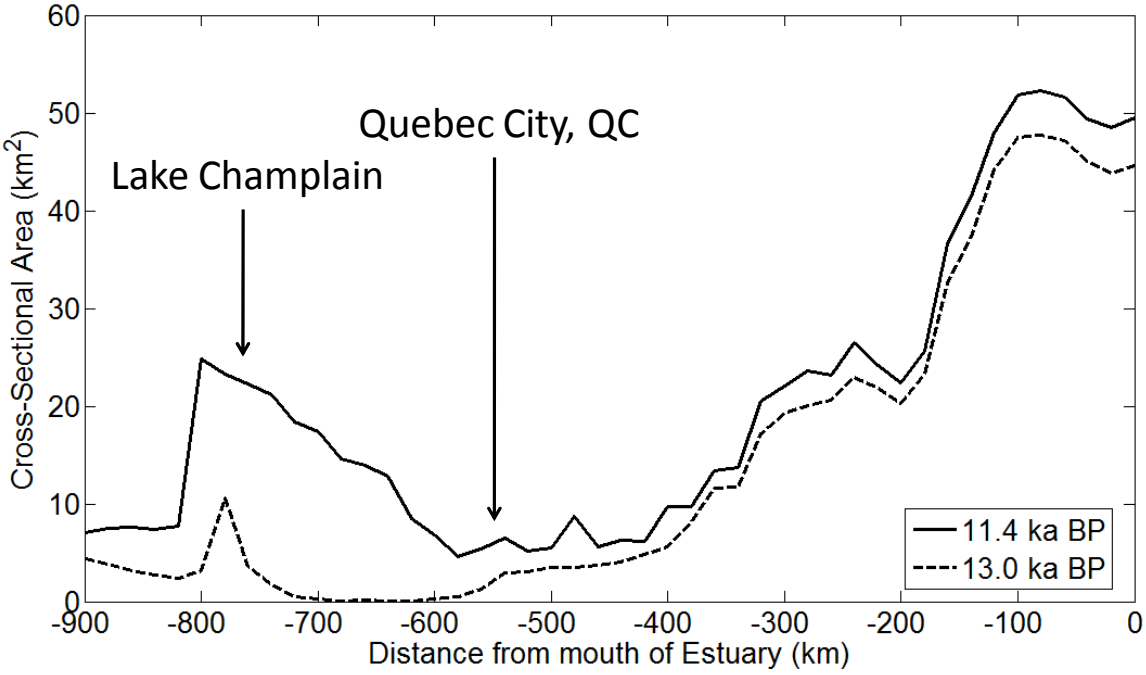

Figure **2.3**: Along-axis cross-sectional area of the estuary for the 11.4 and 13.0 ka BP scenarios. The current-day location of Lake Champlain and Quebec city are shown.

2.3 Estuarine Model Forcings

For the model to simulate steady-state, pre-flood conditions, information about baseline (i.e. pre-flood) freshwater flow, ocean boundary salinity, and daily averaged tidal velocity are needed. Baseline freshwater flows of 34,000 and 47,000 m^3s^{-1} for the 11.4 and 13.0 ka BP scenarios, respectively, are acquired from Teller et al. (2002). These values are derived from knowledge on the Laurentide Ice Sheet and its melt rates, extensive field mapping of the Agassiz shorelines and sediments, and estimates on the total volume of pro-glacial Lake Agassiz, the source of freshwater to the Champlain Sea.

The value for salinity at the ocean boundary is assumed to be constant at 30 ppt, similar to the current-day annual-mean salinity in the Gulf of St. Lawrence (Koutitonsky et al. 2002).

Using the estimates for baseline freshwater flow and ocean boundary salinity, the daily averaged tidal velocity, which is poorly known for the past, may then take the place of a tuning parameter. The tidal velocity is varied until the salinity at the location of the core-derived data equals the observed value (≈ 25 ppt, see section 2.4 below). With initial conditions satisfied, the model is then run using varying flood magnitudes and durations derived from the geologic evidence presented in the next section.

2.4 Observed Salinity and Flood Volume Constraints

Studies of Champlain Sea paleo-salinity have been conducted for more than a century (Cronin et al. 1977, Rodriguez and Vilks 1994). These studies have primarily used faunal assemblages (benthic foraminifers and ostracodes) (Cronin 1979, Hunt and Rathburn 1988, Guilbault 1989, 1993, Rodrigues 1992) and stable isotopic values on benthic foraminiferal $CaCO_3$ shells (Corliss et al. 1982, Cronin et al. 2008a) within the cores. The combination of stable isotopic analysis with the forminiferal assemblages allows for relatively accurate information on paleo-salinity changes within the Champlain Sea. Within the record, several fresh and marine oscillations have been noted; however this study will only focus on the 11.4 and 13.0 ka BP events, as they are two of the largest freshening events in the Champlain Sea geologic record and are likely linked to Lake Agassiz and Algonquin freshwater drainage pulses.

The 11.4 ka BP freshening event was most recently studied by Cronin et al. (2008a). The cores obtained in this study indicate a change from marine to brackish water conditions, from about 25 ppt to 8 ± 3 ppt. All of the cores collected by Cronin et al. (2008a) in and around the current-day Lake Champlain contain evidence of this freshening, allowing confidence to be placed on magnitude and timing of this freshwater flood event. The 13.0 ka BP event also has a

complex, well-studied history, beginning with the study performed by Cronin (1977) to the present day with the work on faunal assemblages by Franzi et al. (2007), Rayburn et al. (submitted), and Cronin et al. (2008b). This event is composed of a complex series of events following the drainage of Lake Vermont and the inundation of the basin with the marine waters of the Champlain Sea. After the marine water entered the region, the microfaunal and stable isotopic evidence indicates a return to fresh and brackish water over a period of decades. It was hypothesized that there was a complete freshening, from 25 ppt to fresh conditions (0 ppt) over decades or less.

The Champlain Sea was coeval with pro-glacial Lake Agassiz in the western plains. During the lifetime of Lake Agassiz, it is observed from paleo-strandlines and the sampling of geologic formations that water level changed drastically during the time events of interest. It is assumed that all of the water lost during these lake level drops drained into the Champlain Sea. Teller et al. (2002) provide estimates for the flood volumes during the 11.4 and 13.0 ka BP events: 3,700 km^3 and 9,500 km^3, respectively.

2.5 Experiment Set Up

In order to test the full parameter space of salinity change vs. flood duration and magnitude, many runs are performed for each event (11.4 and 13.0 ka BP). The first set of runs use the estimated flood volumes of Teller et al. (2002) spread out evenly over times of one day, two days, seven days, fourteen days, and one to twelve months (A total of 16 time periods for each event). The total flood volume is then increased and decreased by factors of 10 and 20 (a total of 5 flood volumes for each event). Thus a total of 5 × 16 = 90 simulations are conducted for each event.

Chapter 3

Results and Discussion

3.1 Pre-Flood Simulations

For the 11.4 and 13.0 ka BP cases, tidal velocities at the mouth of the estuary equal to 3.05 and 0.25 ms^{-1}, respectively, are required to create steady-state conditions in the Champlain Sea such that, at the location where core-derived paleo-salinity information is present, the vertically averaged paleo-salinity equals the value suggested by Cronin et al. (2008a), approximately 25 ppt for both cases. Figure 3.1 shows the simulated steady-state paleo-salinity and velocity fields in the Champlain Sea. The 11.4 ka BP simulation has the characteristics of a partially mixed estuary, like Chesapeake Bay, with a landward flow at depth and a seaward flow near the surface. Salinity increases smoothly with depth and with distance towards the ocean. The pattern is remarkably similar to that hypothesized for the Champlain Sea by Rodrigues and Vilks (1994; their figure 14). Results for the simulation at 13.4 ka BP are similar except that there is an unexpected minimum in surface salinity located approximately 500 to 700 km from the mouth of the estuary. This fresh pool coincides with a very shallow and narrow region of the estuary, and is likely an artifact of the estuarine model's parameterization of the vertical paleo-salinity profiles. Similar behavior can be seen in all areas where sharp changes in bottom topography occur. This unexpected behavior will be discussed in greater detail below.

By using the bathymetry, tidal velocities, and forcings noted above, the model may now be run forward in time for the tests noted in section 2.5.

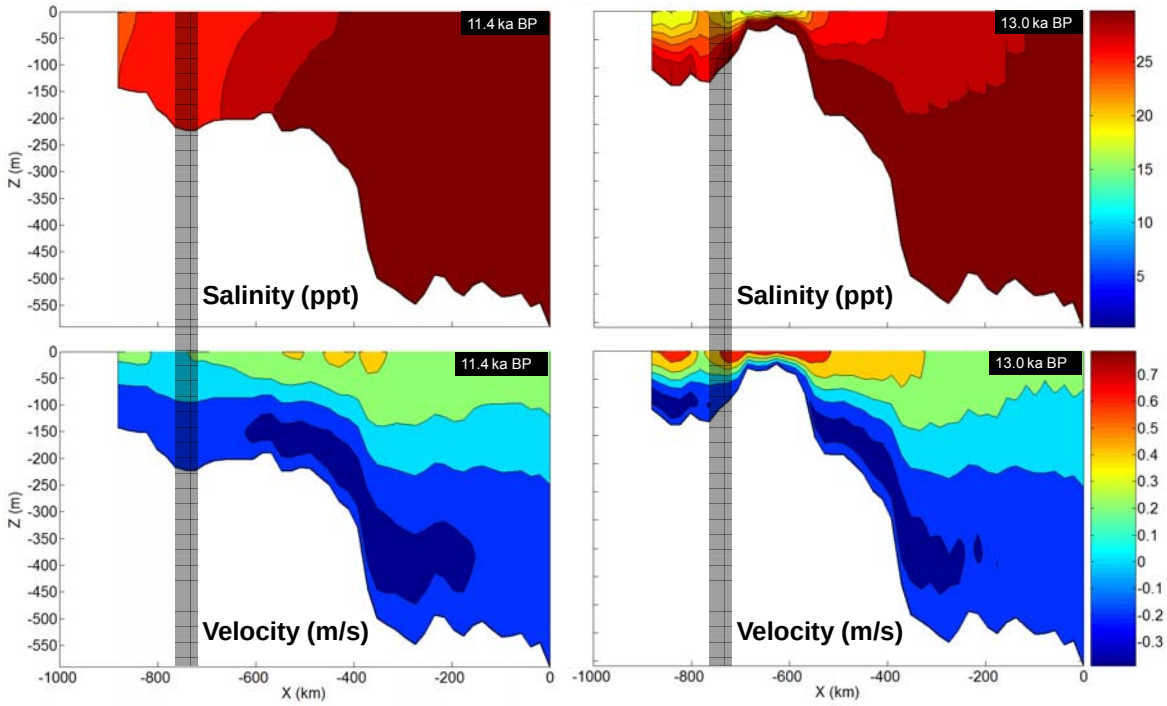

Figure **3.1**: Steady-state conditions in the Champlain Sea for the 11.4 (left) and 13.0 (right) ka BP scenarios. The top images display paleo-salinity in ppt, while the bottom images show the steady state velocity in m s^{-1}. The highlighted area is the location where Cronin et al. (2008a) have taken core data.

3.2 Simulations of the 11.4 ka BP Event

According to Cronin et al. (2008a), the total paleo-salinity decrease during the 11.4 ka BP event may have been as high as 17 ppt. Although it is difficult to calculate error bars on this paleo-salinity change using $\delta^{18}O$ values due to the lack of an extant Champlain Sea today, Cronin et al. (2008a) were able to combine information on faunal assemblages and stable isotopic data from adjacent measurements to estimate an accuracy of $\pm$ 3 ppt.

The first simulations presented use the total freshwater flood volume suggested by Teller et al. (2002): 3,700 km^3. The model is allowed to run for 80 days prior to the flood to ensure that a steady-state solution has been reached. Figures 3.2 (a) and (b) show the evolution of vertically averaged salinity at the core location for a scenario in which the entire 3,700-km^3 flood volume is released equally over 1 day and over 2 months, respectively. The maximum salinity drop is 13 ppt for the 1-day flood and 8 ppt for the 2-month flood. One can clearly see that salinity drops as soon as the flood begins and approaches the pre-flood value in a quasi-exponential manner immediately after the flood ends. A rough estimate of the characteristic response time (or *e*-folding time) for returning to pre-flood salinity (S_p = 25 ppt) can be made by determining the time it takes the salinity to go from its minimum value ($S_m$to $S_p - (S_p - S_m)e^{-1}$. For the 1-day and 2-month floods the response times are 33 and 39 days, respectively. The response time for the salinization of the estuary after the flood event apparently decreases with flood duration. This makes sense as the residual circulation of an estuary increases with the volumetric flow rate of its freshwater forcing; a stronger residual circulation means a shorter residence time for water parcels in an estuary and therefore a more rapid return to steady state.

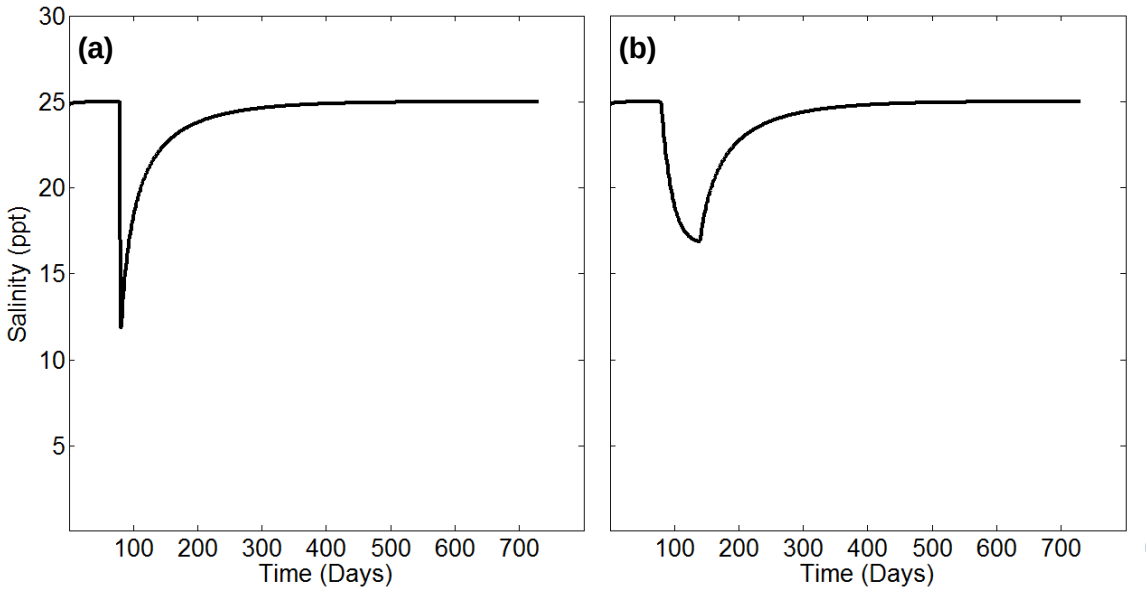

Figure **3.2**: Depiction of vertically averaged paleo-salinity over time at the core location for a 3,700-km^3 flood equally spread out over 1 day (a) and 2 months (b).

Figure 3.3 shows the paleo-salinity and flow estimations for the estuary on the day of the large 1-day flood depicted in figure 3.2 (a). Note the large change in the surface paleo-salinity (down to about 100 m depth) while the bottom paleo-salinity remains largely unchanged (compare with the left side of figure 3.1). This behavior is mimicked in all of the model runs, and may provide insight into the way in which the vertical profile of paleo-salinity is affected by these large floods. As in most estuaries, short-term flow increases only freshen the surface layer, while the more dense and salty bottom layer remains largely unchanged. Given more time with sustained freshwater flow increases, the larger concentration of salt in the bottom layer slowly erodes away as water is exchanged across the fresh/salty boundary at around 100 m depth. This behavior can be seen in the model run summary results in figure 3.4 as 1-day floods tend to have less vertically averaged paleo-salinity decreases than 2-day floods, which have more time to erode at the salt boundary.

The flow velocity changes are also very dramatic, particularly in surface waters, where flow velocities reach about 10 m s^{-1}, values that are rarely, if ever, reached in modern estuaries. The magnitude of this flood, however, has no modern analog, amounting to a flow rate of more than 40 × 10^6 m^3 s^{-1}, or 40 Sverdrups. It should be noted, however, that limitations within the estuarine model make the results only suggestive of what such a large flood would produce, if only because the model has not been evaluated with such high flow rates. Further, floods of this volume would likely have a dramatic impact on bottom topography. The estuarine model used here (MacCready 2007), however, like many estuarine circulation models, has fixed bathymetry. More discussion of the errors associated with the estuarine model for this application will be discussed below.

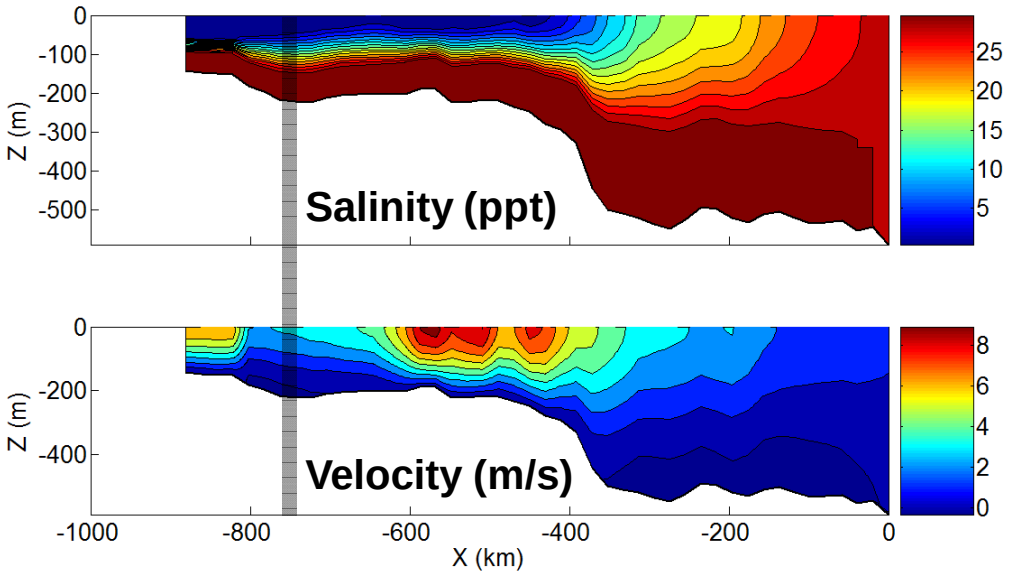

Figure **3.3**: Model salinity and velocity at the onset of the 1-day 3,700-km^3 flood. The highlighted area is the location of cores from Cronin et al. (2008a).

Figure 3.4 below displays the summary results for all of the 11.4 ka BP runs. By assuming that the lower bound of paleo-salinity change is valid (14 ppt), it can be seen that total flood volumes between 5,500 km^3 and 10,000 km^3 can yield a total paleo-salinity change within the range inferred from the core-derived paleo-salinity data. These floods would have to occur relatively quickly, on the order of 10 days or less, in order to cause the suggested paleo-salinity decrease. To put these flood volumes into perspective, the maximum estimated total volume of Lake Agassiz around the time of these floods would have been approximately 20,000 km^3, while the flood volume suggested by Teller et al. (2002) for this time period is only 3,700 km^3. If it is assumed that Lake Agassiz drained completely during this time, the maximum possible change is only 17 ppt. If it is again assumed that the lower bound value of paleo-salinity change (14 ppt) is possible, the maximum duration of a 20,000 km^3 flood is approximately 45 days. Although it is possible that Lake Agassiz drained completely during this time, it is more likely that the total flood amount was considerably less, leading to the conclusion that a flood moving through this estuary did so on the order of days or weeks, not months or years.

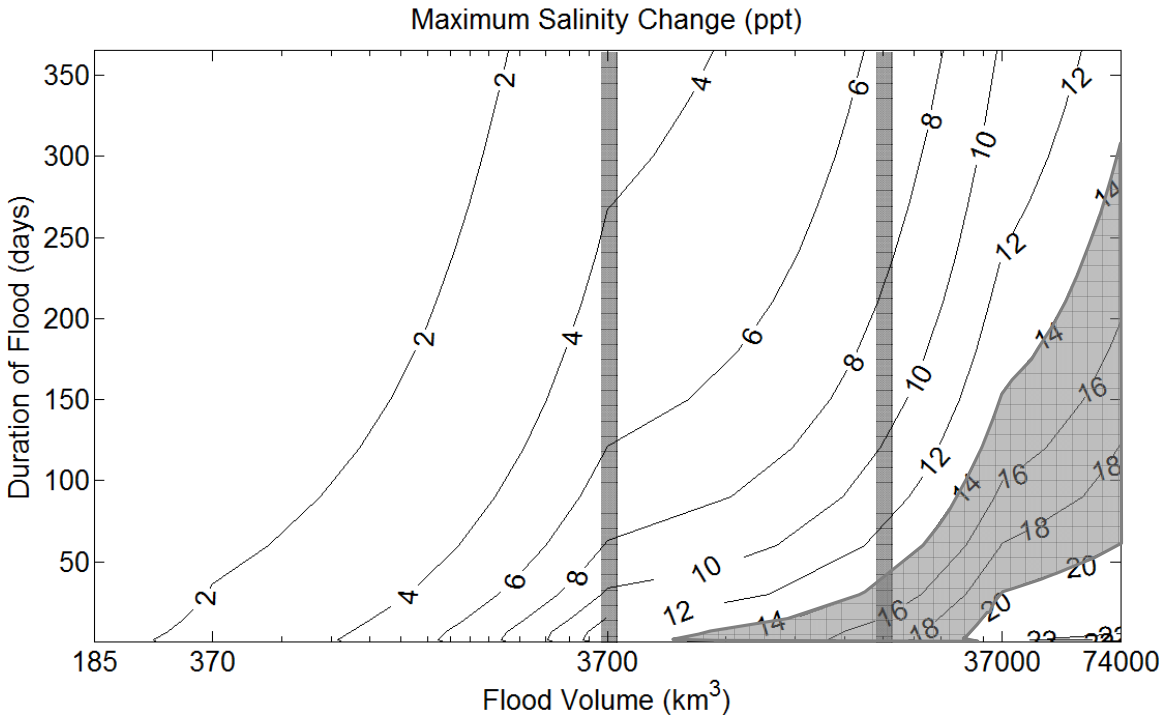

Figure **3.4**: Summary results for the 11.4 ka BP scenario where a change in paleo-salinity of 17 ± 3 ppt is expected. This image shows how varying flood volumes (x-axis) and durations (y-axis) affect the vertically averaged paleo-salinity at the location of the core information (displayed in figure 3.1 as the shaded region). The shaded polygon shows the uncertainty of the paleo-salinity change as obtained from Cronin et al. (2008a), ± 3 ppt. The left and right shaded columns represent the flood volumes of 3,700 km^3 and 20,000 km^3 respectively.

3.3 Simulations of the 13.0 ka BP Event

During the 13.0 ka BP freshening event, Cronin et al. (2008a) suggest that a total freshening of the Champlain Sea occurred, a paleo-salinity change of 25 ppt. The summary results of the 13.0 ka BP runs are shown in figure 3.5. This analysis is subject to the same error as the 11.4 ka BP case, with error bars of ± 3 ppt. However, because the analysis of the model results did not contain any instances of a 25 ± 3 ppt paleo-salinity change, there is no highlighted area on this figure. This result may mean one of several things: that the Champlain

Sea did not totally freshen during this time period, that the bathymetry was not properly reconstructed, that there were source of freshwater other than Lake Agassiz to the Champlain Sea, or that limitations in the estuarine model used prevented a correct solution from being obtained.

Although the bathymetries of the 11.4 and 13.0 ka BP cases are relatively dissimilar, it should be noted that the total volumes only differ by about 30%, with the 11.4 ka BP case having a larger overall volume. If bathymetry is ignored, then it should take more freshwater to change the paleo-salinity in the 11.4 ka BP case than in the 13.0 ka BP case. However, the opposite relationship is seen. As will be shown below, there are several possible sources of error in the reconstruction of the bathymetry, particularly for the 13.0 ka BP case.

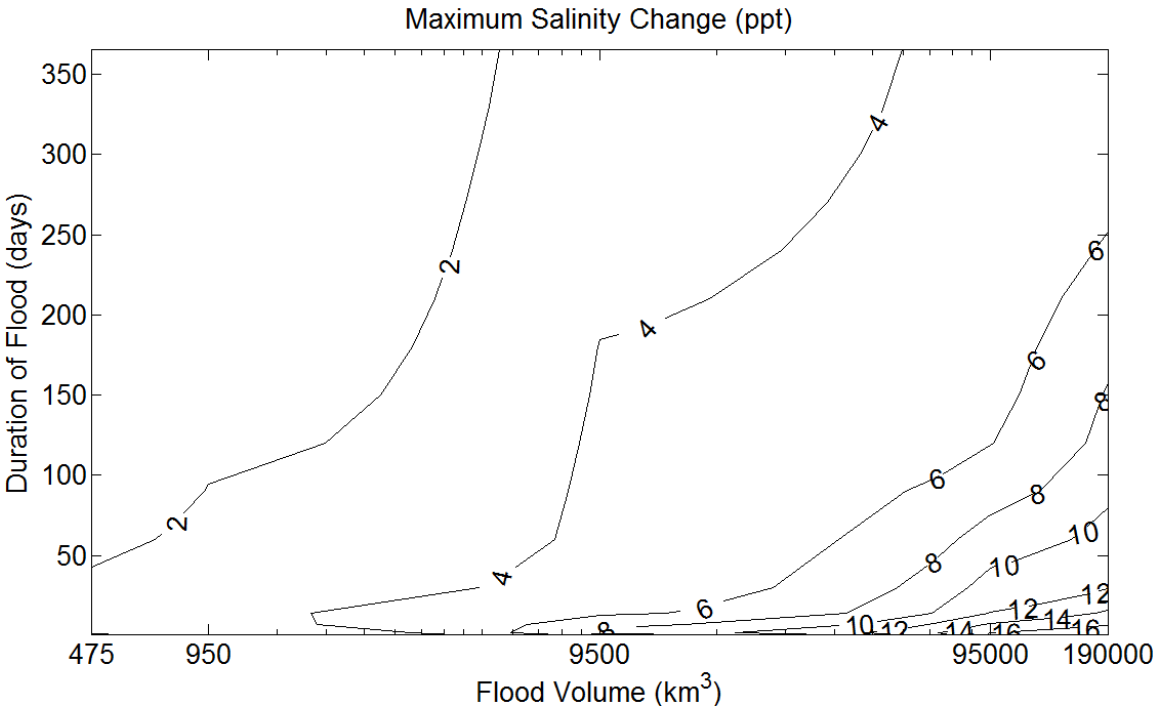

Figure **3.5**: Summary results for the 13.0 ka BP scenario. This image shows how varying flood volumes (x-axis) and durations (y-axis) affect the vertically averaged paleo-salinity at the location of the core information (displayed in figure 3.1 as the shaded region). There is no shaded polygon due to the fact that the observed change in paleo-salinity of 25 $\pm$ 3 ppt is not present.

3.4 Possible Sources of Error

There are several possible sources of error within the above experiment. Errors stem primarily from the construction of the bathymetry and include: under and over estimations of depth in the current-day DEM, assumptions used in the creation of the paleo-DEM, the method of combination of the maps, the estimation of the true depth of the waterway, and the location of the southern extent of the Laurentide Ice Sheet. Other sources of error are attached to the estuarine model and the assumptions inherent in its construction.

The current-day DEM has a relatively coarse grid consisting of 2 x 2 km boxes. Because of the averaging of the topography within each of these boxes, it is likely that over and under-estimations of the true elevation are present within the bathymetric analysis performed above. This is due to the fact that sharp dips and peaks within each grid box will be smeared out when elevations within the box are averaged. The over and under estimations of the true area of each transect may be somewhat mitigated, however, due to the fact that there is a nearly equal likeliness of recording data for elevations that are above and below the correct value.

The paleo-DEM of the western Champlain Sea constructed by Rayburn et al. (2005) also contains error due in large part to the methods and data used in its construction. Because the land reconstruction model is primarily based on paleo-strandlines, which provide information on the coastlines (and therefore depth), and isostatic rebound lines, which provide information on how different areas rebound after having the weight of the Laurentide Ice Sheet removed, the final product is subject to measurement and calculation uncertainty. Also, the mathematical models used to simulate isostatic rebound are based on the current-day configuration of Lake Champlain, and may not properly account for land formation changes caused by thousands of years of erosion and sedimentation. Unfortunately, it is difficult to quantify this error in any useful way, or even to determine its sign.

In combining the nautical charts, the current-day DEM, and the paleo-DEM, the method described in figure 2.1 was used. Combining the nautical chart with the current day DEM requires that this operation be carried out for each transect, and error is likely linked very closely to the coarse resolution of the current-day DEM. Because the nautical chart and the current-day DEM both depict the same area at roughly the same time, the relative elevations should require no correction. However, because the current-day DEM averages the elevations

within each grid box, the boxes at the coasts where the maps are connected may see elevation disparities on the order of 1 to 30 m. This is likely caused by the fact that coastal regions are often areas of sharp elevation increase, which, as was mentioned before, are washed out due to the DEM box averaging. In this case, error is likely negative in sign, due to the fact that the current-day DEM cross-sections to the north and south of the coasts are corrected for an elevation that is underpredicting the true elevation due to the averaging out of sharp coastal elevation increases.

The operation inherent in the connection of the paleo-DEM maps with the nautical chart/current-day DEM provides another source of error. Although the operation used to connect the data sets together is identical to the method used to tie the nautical charts to the current-day DEM, the purpose for doing so is different. Performing the aforementioned correction is a simplistic way of modeling isostatic rebound wherein the current-day maps are uniformly corrected, on the order of -150 m, to the level of the northeastern point in the paleo-DEM. The error inherent in using this uniform correction factor may not be as big as anticipated due to the curvature of the isostatic rebound lines in the St. Lawrence, which follow the coastline of the waterway (Parent and Occhietti, 1988). This means that the land along the St. Lawrence rebounded at roughly the same rate as the northeastern point in the paleo-DEM used to correct the current-day maps. Because the rebound rates are more to the north and less to the south of this isostatic rebound line, the error inherent in the uniform correction likely cancels out, with the remaining error being only on the order of a couple meters of indeterminate sign.

After combining all the maps to obtain consistent bottom topography, a free water surface must be overlaid on the data set in order to determine the depth of the water. Rayburn

et al. (2005) provide an estimate for the location of the free water surface for the paleo-DEM based on the strandlines mentioned earlier. After combining the paleo-DEM with the current-day maps, this free water surface is used for the entire data set. The error caused by this assumption is due to the fact that the mean free water surface slopes downward from the head to the mouth of an estuary. This is somewhat accounted for in the usage of the nautical charts for depths in the St. Lawrence. The nautical chart data come from ship soundings along the waterway, which inherently sample the true depth and therefore include the increase in relative elevation moving upstream into the estuary.

The final primary source of error in the bathymetry is the location of the southern boundary of the Laurentide Ice Sheet. The latitude and longitude locations of the southern boundary of the ice sheet obtained from Dyke et al. (2008) were only available in increments of 500 Radiocarbon years (a timescale which does not match up with the calendar years of the events studied above), and do not coincide with the time periods used in the paleo-DEMs. Because the time periods of interest lie in-between the data available, the older data were subsequently always chosen. This was done so that the ice sheet was always at its most southerly position, creating a situation such that the sign of the error was always negative. In other words, the ice sheet is always further south than the true location during this time. For the 11.4 ka BP situation, this error is very small due to the fact that the northern boundary of the waterway is mostly made up of land for both the older and younger locations for the ice sheet. However, the difference between the location of the older and younger southern boundary of the ice sheet for the 13.0 ka BP situation is very different, with nearly the entire northern boundary of the waterway bounded by the ice sheet. This is likely the largest error due to the bathymetry, and is a primary area for future study as small changes in the southern

extent of the ice sheet along the estuary can significantly change the depth and cross-sectional area of the water-way.

Within the estuarine model itself, there are other sources of error. MacCready (2007) states that this model has difficulty in areas where the bottom topography varies greatly over small distances and in places where the waterway is very narrow and shallow. While this does not occur as much in the 11.4 ka BP case, the 13.0 ka BP case has an area of narrow, shallow waters about midway up the estuary. This bottleneck within the 13.0 ka BP model is likely responsible for this case's low average daily tidal velocity, which is an order of magnitude less than that of the 11.4 ka BP case; this low tidal velocity is needed to increase the intrusion length of salinity to obtain the correct initial conditions stated above. Due to this smaller tidal velocity, it is more difficult to flush salty water out of the estuary, and the results of the 13.0 ka BP model may be more salty than expected. It is difficult to determine if this is an artifact of the model or a real attribute of the system during this time period. It does however seem quite unlikely that tidal velocities should change by more than an order of magnitude between the 11.4 and 13.0 ka BP scenarios. Furthermore, the unexpected paleo-salinity minimum seen in the pre-flood simulation (figure 3.1) is strongly suggestive that the estuarine model is not producing realistic results for the 13.0 ka BP case.

Chapter 4

Conclusion

The above analysis represents a useful approach to quantifying the forcings responsible for observed changes in the geologic record and may provide useful information for those attempting to model the effect of large freshwater injections into the North Atlantic. The location of the core-derived salinity data obtained by Cronin et al. (2008a) is useful in this respect as it implies that the freshwater floods likely flowed out of the current-day Gulf of St. Lawrence and into the primary zone of NADW formation (Sarnthein et al. 1994). Understanding the duration and magnitude of these freshening events is essential to modeling the formation of NADW, a key component of the MOC, which is known to have drastic effects on climate. The 13.0 ka BP scenario is of particular interest as it closely predates the onset of the Younger Dryas Cooling Event and may have had a significant impact on the MOC. It is therefore useful to add constraints on the magnitudes, durations, and timings of these large freshening events.

This study has additional utility in that the results garnered may be used to better constrain the timing of the major stage changes of Lake Agassiz. While the results for the 13.0 ka BP run proved inconclusive, the 11.4 ka BP runs provide motivation for re-examining either the timing or magnitude of the flood events as described by Teller et al. (2002) due to the larger volume needed to cause the observed salinity changes. Performing this study on a larger subset of paleo-salinity derived freshening events, and then ranking the flood volumes needed to make the required salinity changes, may allow more definite assertions to be made as to the correct timing of the flood events. This type of chronology is useful due to the relatively accurate timing of events in the Champlain region, which can be correlated to lake-stage changes in Agassiz.

While useful, this study contains several sources of error, which may decrease confidence in the results. To decrease uncertainty, better constraints on the bathymetry are required. Combining three different map sources into one is far from ideal, and it is difficult to quantify the errors incurred by doing so. A re-creation of the entire estuary, from current-day Lake Erie to the Gulf of St. Lawrence, would substantially increase the accuracy of the results. In addition, obtaining more accurate locations for the southern boundary of the Laurentide Ice Sheet by increasing the temporal resolution of the locations by Dyke et al. (2008) is critical to understanding older events (e.g., 13.0 ka BP) wherein the ice sheet forms the northern boundary of the waterway. If these data are unavailable, interpolation of the location of the southern boundary between data sets may be performed.

Perhaps the most important improvement to the study would be to choose a more appropriate estuarine model. While the results for the 11.4 ka BP scenario were within the bounds of the model limitations, the sharp changes in the bathymetry of the 13.0 ka BP scenario caused artifacts in the results, such as the severely decreased tidal velocity, as well as the salt and flow anomalies mentioned in Chapter 3. A model that fully resolves the two-dimensional equations of motions, instead of one which uses parameterizations based on unavailable variables (due to the fact the estuary does not exist today), would be advantageous. Going further, a three-dimensional wettable finite element model may also be better suited to this analysis, as it accounts for twists and turns in the primary flow axis and inundation of water into the surrounding land area above the coastlines.

Though substantial error in this study exists, it is still a useful exercise as it provides fair estimates of flood volume and duration for situations where bathymetry is relatively smooth. Performing the above analysis for more events will likely yield very useful results. For situations

where uncertainly remains in the construction of the bathymetry, such as the 13.0 ka BP event, analysis should be performed wherein the younger ages for the southern extent of the Laurentide Ice Sheet are chosen. This will lead to well-behaved bathymetries which in turn will allow useful results to be gained. In this way, a chronology of flood volumes may be recorded for use in future studies.

Bibliography

Amante, C. and B. W. Eakins, ETOPO1 1 Arc-Minute Global Relief Model: Procedures, Data Sources and Analysis, National Geophysical Data Center, NESDIS, NOAA, U.S. Department of Commerce, Boulder, CO, August 2008.

Broecker, W., Kennett, J., Flower, B., Teller, J., Trumbore, S., Bonani, G., and Wolfli, W., 1989. Routing of Meltwater from the Laurentide Ice Sheet During the Younger Dryas Cold Episode. Nature (London) **341**, 318–321.

Geology Map of New York: Adirondack Sheet. New York Museum Map and Chart Series **40**, Scale 1:250,000.

Corliss, B., Hunt, A., Keigwin Jr., K., 1982. Benthonic Forminiferal Faunal and Isotopic Data for the Postglacial Evolution of the Champlain Sea. Quaternary Research **17**, 325-338.

Cronin, T., 1977. Late-Wisconsin Marine Environments of the Champlain Valley: New York, Quebec. Quaternary Research **7**, 238–253.

Cronin, T., 1979. Late Pleistocene Benthic Foraminifers from the St. Lawrence Lowlands. Journal of Paleontology **53**, 781–814.

Cronin, T., Manley, P., Brachfeld, S., Manley, T., Willard, D., Guilbault, J., Rayburn, J., Thunell, R., Berke, M., 2008a Impacts of Post-Glacial Lake Drainage Events and Revised Chronology of the Champlain Sea Episode 13-9 ka. Paleogeography, Paleoclimatology, Paleoecology **262**, 46-60.

Cronin, T., Rayburn, J., Thunell, R., Guilbault, J., Katz, B., Najjar, R., Manley, P., 2008b. North American Glacial Lake Drainage through the St. Lawrence Estuary from 13 to 9 ka. Fall AGU Meeting 2008 San Francisco, PP51E-05.

Dyke, A., 2008. Deglaciation of North America. Natural Resources of Canada, http://ess.nrcan.gc.ca/ercc-rrcc/proj6/index_e.php.

Franzi, D., Rayburn, J., Knuepfer, P., Cronin, T., 2007. Late Quaternary History of Northeastern New York and Adjacent Parts of Vermont and Quebec. 70th Annual Northeast Friends of the Pleistocene Guidebook. Plattsburgh, New York (70 pp.).

Ganopolski, A., Rahmstorf, S., 2001. Rapid Changes of Glacial Climate simulated in a Coupled Climate Model. Nature **409**, 153-158.

Guilbault, J., 1989. Forminiferal Distribution in the Central and Western Parts of the Late Pleistocene Champlain Sea Basin, Eastern Canada. Géographie Physique et Quatemaire **43**, 3-26

Guilbault, J., 1993. Quaternary Forminiferal Stratigraphy in Sediments of the Eastern Champlain Sea Basin, Québec. Géographie Physique et Quatemaire **47**, 43-68

Hansen, D., Rattray, M., 1965. Gravitational Circulation in Straits and Estuaries. J. Mar. Res., **23**, 104-122.

Hunt, A., Rathburn, A., 1988. Microfaunal Assemblages of Southern Champlain Sea Piston Cores. The Late Quaternary Development of the Champlain Sea Basin. Geological Association of Canada Special Publication **35**, 145-154.

Koutitonsky, V., Navarro, N., Booth, D., 2002. Descriptive Physical Oceanography of the Great-Entry Lagoon, Gulf of St. Lawrence. Estuarine, Coastal and Shelf Science **54**, 833-847.

Leverington, D., Teller, J., 2003. Paleotopographic Reconstructions of the Eastern Outlets of Glacial Lake Agassiz. Can. J. Earth Sci. **40**, 1259-1278.

Lowell, T., Fisher, T., Comer, G., Hajdas, I., Waterson, N., Glover, H., Loope, H., Schaffer, J., Rinterknecht, V., Broeker, W., Denton, G., Teller, J., 2005. Testing the Lake Agassiz Meltwater Trigger for the Younger Dryas. EOS **86**, 365-373.

MacCready, P., 2007. Estuarine Adjustment. J. Phys. Oceanogr. **37**, 2133-2145.

Parent, M., Occhietti, S., 1988. Late Wisconsoninan Deglaciation and Champlain Sea Invasion in the St. Lawrence Vallyey, Québec. Géographie Physique et Quatemaire **53**, 117-135.

Peltier, W., Fairbanks R., 2006. Global Glacial Ice Volume and Last Glacial Maximum Duration from an Extended Barbados Sea Level Record. Quaternary Science Reviews **25**, 3322-3337.

Pirazzoli, P., Pluet, J., 1991. World Atlas of Holocene Sea-Level Changes. Elsevier Oceanogr Ser 58. Elsevier, Amsterdam, 300

Press, W., Teukolski, S., Vetterling, W., Flannery, B., 1992. Numerical Recipes in C: The Art of Scientific Computing. 2d ed. Cambridge University Press, 994.

Rayburn, J., Kneupfer P., Franzi D., 2005. A Series of Large, Late Wisconsonian Meltwater Floods through the Champlain and Hudson Valleys, New York State, USA. Quaternary Science Reviews **24**, 2410-2419.

Rayburn, J., Verosub, K., Franzi, D., Knuepfer, P., 2006. A Preliminary Paleomagnetic Study of the Glacial Lacustrine/Champlain Sea Transition in Cores from the Northern Champlain Valley, New York. Geological Society of America, Abstracts with Programs Northeastern Section **38**, # 2.

Rayburn, J., Franzi, D., Kneupfer, P., 2007. Evidence from the Lake Champlain Valley for a Later Onset of the Champlain Sea and Implications for Late Glacial Meltwater Routing to the North Atlantic. Paleogeography, Paleoclimatology, Paleoecology **246**, 62-74.

Rayburn, J., Cronin, T., Franzi, D., Knuepfer, P., Willard, D., submitted. Timing and Duration of Glacial Lake Discharges and the Younger Dryas Climate Reversal.

Rodrigues, C., 1988. Late Quaternary Invertebrate Faunal Associations and Chronology of the Western Champlain Sea Basin. Geological Association of Canada Special Paper **35**, 155-176

Rodrigues, C., 1992. Successions of Invertebrate Microfossils and the Late Quaternary Deglaciation of the Central St. Lawrence Lowland, Canada and the United States. Quaternary Science Reviews **11**, 503-534.

Rodrigues, C.G., Vilks, G., 1994. The Impact of Glacial Lake Runoff on the Goldthwait and Champlain Seas: The Relationship Between Glacial Lake Agassiz Runoff and the Younger Dryas. Quaternary Science Reviews **13**, 923–944.

Sarnthein, M., Winn, K., Jung, S., Duplessy, J., Labeyrie, L., Erlenkeuser, H., Ganssen, G., 1994. Changes in Easy Atlantic Deepwater Circulation over the Last 30,000 Years: Eight Time Slice Reconstructions. Paleo-Oceanography **9**, 209-267.

Teller, T., Leverington, W., Mann, J., 2002. Freshwater Outbursts to the Oceans from Glacial Lake Agassiz and their Role in Climate Change during the Last Deglaciation. Quaternary Science Reviews **21**, 879-887.

Teller, J., Leverington, D., 2004. Glacial Lake Agassiz: A 5000 yr History and its Relationship to the $\delta^{18}O$ Record of Greenland. GSA Bulletin **116**, 729-742.

Appendix

Nautical Chart References

Table **D-1**: Nautical Charts from The Defense Mapping Agency Hydrographic/Topographic Center in Bethesda, MD

Map ID #	Edition	Publication Year
14260	44th	1984
14223	18th	1995
14225	17th	1995
14226	32nd	1995
14227	28th	1995
14228	11th	1995
14240	6th	1995
14241	23rd	1995
14242	13th	1995
14243	8th	1995